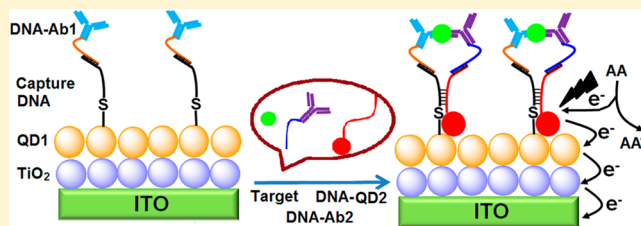


## Enhanced Photoelectrochemical Proximity Assay for Highly Selective Protein Detection in Biological Matrixes

Guangming Wen<sup>†,‡</sup> and Huangxian Ju<sup>\*,†</sup><sup>†</sup>State Key Laboratory of Analytical Chemistry for Life Science, School of Chemistry and Chemical Engineering, Nanjing University, Nanjing 210023, P.R. China<sup>‡</sup>School of Chemistry and Chemical Engineering, Shanxi University, Taiyuan 030006, P.R. China

## Supporting Information

**ABSTRACT:** This work proposes the first photoelectrochemical proximity assay (PECPA) method via the sensitization of CdTe quantum dots (QDs) on photoelectrochemical response of ITO/TiO<sub>2</sub>/CdS electrode for highly selective and sensitive detection of proteins. This detection was performed on a sensing interface formed via the hybridization of capture DNA immobilized on ITO/TiO<sub>2</sub>/CdS electrode with labeled antibody-DNA (DNA-Ab1). Upon the recognition of Ab1 to target protein, the immunocomplex of DNA-Ab1, target, and the detection antibody-DNA (DNA-Ab2) was formed, which led to the proximity hybridization of the DNA in DNA-Ab2, capture DNA, and signal DNA-CdTe QDs, and brought CdTe QDs to the ITO/TiO<sub>2</sub>/CdS electrode to produce a sensitized photocurrent. The photocurrent intensity increased with the increasing concentration of the specific target protein. Using insulin as a target, this sensitized method showed a detectable range of 10 fM to 10 nM and a detection limit of 3.0 fM without the need of a washing step. It possessed high selectivity and good accuracy for detection of proteins in biological matrixes. This method is extremely flexible and can be extended to varieties of protein targets.



Specific protein detection is very important in health care and medical treatment, since it is one of the simplest methods to diagnose the onset or progression of disease states.<sup>1,2</sup> Immunoassay is one of the dominant methods for specific protein detection due to the highly specific molecular recognition. However, it is difficult to realize point-of-care detection via conventional immunoassays.<sup>3</sup> Recently, DNA-assisted protein detection methods have been developed for clinical diagnosis, environmental analyses, and food industries.<sup>4–8</sup> In these fields, powerful nucleic acid detection can be used for protein analysis by equipping protein-binding reagents, typically antibody, with DNA strand to improve the analytical performance.<sup>9</sup> As a successful example, immuno-PCR has been performed on a capture antibody immobilized solid-support.<sup>10</sup> After a sandwich immunoreaction, the DNA sequence labeled on the immunocomplex is exponentially amplified by PCR to sensitize the signal of the immune-recognition event.<sup>11–15</sup> Moreover, the sensitivity of immuno-PCR can be further improved by extra signal amplification techniques, including bio barcode.<sup>16</sup> Other DNA amplification strategies, such as hybridization chain reaction and rolling circle amplification, have also been used for highly sensitive detection of protein by in situ amplification.<sup>17–22</sup> However, these assay procedures are multistep, which limits their application in point-of-care detection. Thus, it is necessary to develop more flexible and highly sensitive quantitative methods.

The proximity ligation assay (PLA),<sup>23,24</sup> one of the most easy-to-use and sensitive protein assay methods,<sup>25</sup> can over-

come some of the limitations of the immunoassay methods mentioned above. This assay is generally homogeneous (no washing step) with small sample volume and low detection limit. In the PLA, “proximity effect” relies on the simultaneous recognition of a target molecule via a pair of affinity probes, including aptamer pairs<sup>23</sup> and a variety of antibody pairs.<sup>24</sup> Thus, this technique possesses high selectivity. Moreover, the oligonucleotide tails of the bound probes can be covalently linked via enzymatic ligation for qPCR readout, which assures the high sensitivity of this technique.

Photoelectrochemical (PEC) analysis has attributed considerable attention in rapid and high-throughput biological assays.<sup>26,27</sup> Benefiting from the different energy forms of excitation source (light) and detection signal (current), PEC detection possesses potentially high sensitivity resulted from the low background signals.<sup>28</sup> Besides, advantageously inherited from the electrochemical method, the photoelectrochemical instrument is simple, portable, and inexpensive compared with conventional optical methods.<sup>29</sup> In this technology, photoactive material plays a major role, meanwhile, the PEC sensing system with enhanced photocurrent intensity and less electron–hole recombination is also desirable for highly sensitive detection. To achieve this aim, a sensitized structure, which is composed of the basic photoactive material and two or more sensitizers, is

Received: July 18, 2016

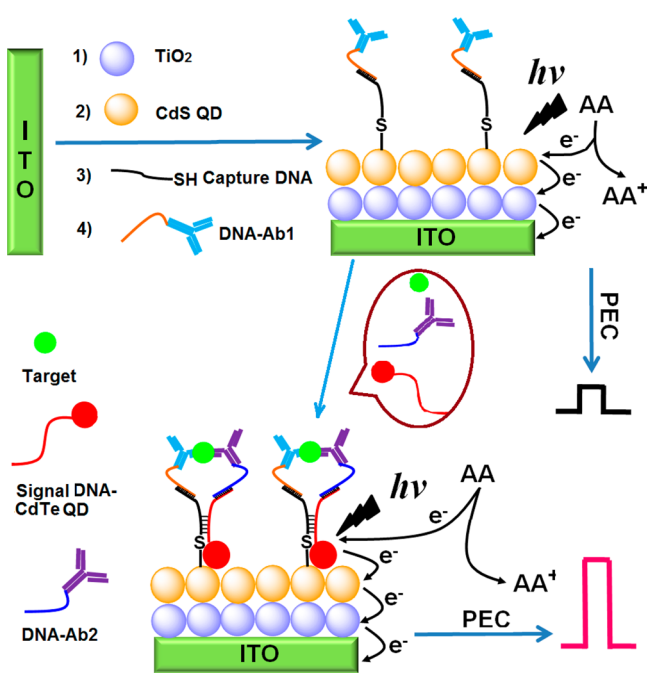
Accepted: July 27, 2016

Published: July 27, 2016

very promising. Considering the different band gaps of different semiconductors, the sensitized structure can be constructed using a couple of the semiconductors with small and large band gaps. The cascade band-edge levels cannot only enhance the photo-to-current conversion efficiency<sup>30</sup> but also facilitate charge separation and therefore enhance the photocurrent density and thus the sensing sensitivity.

On the basis of the sensitization of CdS quantum dots on TiO<sub>2</sub><sup>31,32</sup> and the electrochemical proximity assay,<sup>33,34</sup> we here presented a PEC proximity assay (PECPA) by combining the proximity assay with PEC detection for simple but highly sensitive detection of specific protein. The PEC biosensor was prepared by four steps (Scheme 1): coating TiO<sub>2</sub> nanoparticles,

**Scheme 1. Schematic Representation of Photoelectrochemical Sensor Preparation and the Designed Photoelectrochemical Proximity Assay (PECPA) Strategy for Target Protein Detection**



forming TiO<sub>2</sub>/CdS hybrid structure, assembling capture DNA by the reaction of Cd<sup>2+</sup> and S<sup>2-</sup> ions, and immobilizing DNA labeled antibody probe (DNA-Ab1) by its hybridization with capture DNA on an indium–tin oxide (ITO) electrode. On the biosensor surface, the target protein could induce the formation of immunocomplex among DNA-Ab1, target and detection antibody-DNA (DNA-Ab2) for proximity hybridization of the DNA in DNA-Ab2, and capture DNA and signal DNA-CdTe QDs to bring CdTe QDs to the ITO/TiO<sub>2</sub>/CdS electrode. Because of the sensitization of CdTe quantum dots (QDs) on photoelectrochemical response of ITO/TiO<sub>2</sub>/CdS electrode, the PECPA method contained a signal amplification process. Compared to the pioneering works in proximity ligation immunoassay,<sup>35–39</sup> electrochemical proximity immunosensing with MB-labeled DNA<sup>33,40</sup> and electrochemical protein sensing,<sup>41,42</sup> the proposed sensitization and signal amplification strategy provided a significantly high sensitivity for PECPA of target protein. In view of the advantages of PLA and PEC detection, this method possessed potential application in point-of-care detection.

## EXPERIMENTAL SECTION

**Reagents and Materials.** ITO slices (type JH52, ITO coating 30 ± 5 nm, sheet resistance ≤10 Ω/square), methanol, cadmium nitrate (Cd(NO<sub>3</sub>)<sub>2</sub>·4H<sub>2</sub>O), and sodium sulfide (Na<sub>2</sub>S·9H<sub>2</sub>O) were purchased from Nanjing Chemical Reagent Co., Ltd. (China). TiO<sub>2</sub> powder (P25) was purchased from the Degussa Co. (Germany). Sodium tellurite (Na<sub>2</sub>TeO<sub>3</sub>), sodium borohydride (NaBH<sub>4</sub>), bovine serum albumin (BSA, 98%; EMD Chemicals Inc.), insulin antibodies (clones 3A6 and 8E2; Fitzgerald Industries), and insulin (Sigma-Aldrich). 3-Mercaptopropionic acid (MPA), 1-ethyl-3-(3-(dimethylamino)propyl) carbodiimide hydrochloride (EDC), *N*-hydroxy succinimide (NHS), sulfosuccinimidyl-4-(*N*-maleimidomethyl) cyclohexane-1-carboxylate (SMCC), and tris (2-carboxyethyl)-phosphine (TCEP) were all obtained from Sigma-Aldrich. Ascorbic acid (AA) was purchased from Sinopharm Chemical Reagent Co., Ltd. (China). All other reagents were of analytical grade and used as received. All aqueous solutions were prepared with deionized water (DI water, 18 MΩ/cm), which was obtained from a Milli-Q water purification system. PBS (pH 7.4, 10 mM) containing 0.1 M NaCl was used for preparation of DNA stock solutions. Dithiothreitol (DTT) and oligonucleotides with following sequences (5' to 3') were from Sangon Biotechnology Inc. (Shanghai, China):

signal DNA: **CCACCCTCTCTTTTCCTATCTCTCCCTCGTCCACCATGC**-(CH<sub>2</sub>)<sub>6</sub>-NH<sub>2</sub>;

capture DNA: (G7) HS-**GCATGGT**ATTTTTTCGTT**CGTTAGGGTTCAAATCCGGC**;

capture DNA: (G5) HS-**GCATGA**ATTTTTTCGTT**CGTTAGGGTTCAAATCCGGC**;

capture DNA: (G10) HS-**GCATGGTGAC**ATTTTT CGTT**CGTTAGGGTTCAAATCCGGC**;

DNA1 for Ab1: HS-(CH<sub>2</sub>)<sub>6</sub>-CCCACTAAACCTCAATCC**ACGGGATTGAACCCCTAACG**;

DNA2 for Ab2: **TAGGAAAAGGAGGAGGGTGG**CCCACTAAACCTCAATCC**ACCCACTTAAAC**

Ref DNA: **TAGGAAAAGGAGGAGGGTGG**CCCACTAAACCTCAATCC**ACCCACTTAAAC**

**CTCAATCCACGGGATTGAACCCCTAACG**.

**Apparatus.** A 500 W Xe lamp was used as the irradiation source with the light intensity of 400 μW cm<sup>-2</sup> estimated by a radiometer (Photoelectric Instrument Factory of Beijing Normal University). The photocurrent was recorded on a CHI 660D electrochemical workstation (Shanghai Chenhua Apparatus Corporation, China) through a three-electrode system with a 0.25 cm<sup>2</sup> ITO as working electrode, a Pt wire as counter electrode, and a saturated Ag/AgCl electrode as the reference electrode. The UV–visible (UV–vis) absorption spectra were recorded on a UV-3600 UV–vis spectrophotometer (Shimadzu, Japan). Electrochemical impedance spectroscopy (EIS) was performed on an Autolab potentiostat/galvanostat (PGSTAT 30, Eco Chemie B.V., Utrecht, The Netherlands) via a three-electrode system in 0.1 M KCl solution containing 5.0 mM K<sub>3</sub>[Fe(CN)<sub>6</sub>]/K<sub>4</sub>[Fe(CN)<sub>6</sub>] (1:1) mixture as a redox probe and recorded in the frequency range of 0.01 Hz to 100 kHz with an amplitude of 50 mV. Transmission electron microscopy (TEM) was conducted with a JEOL-2100 transmission electron microscope (JEOL, Japan).

**Preparation of DNA-Labeled Antibody.** The DNA labeled antibody (DNA-Ab) was prepared by a modified coupling procedure.<sup>33,43</sup> At room temperature, anti-insulin (2 mg/mL) reacted with a 20-fold molar excess of SMCC in PBS (pH 7.4) containing 55 mM phosphate, 150 mM NaCl and 20 mM EDTA for 2 h. The obtained anti-insulin-SMCC was purified by ultrafiltration with a 100 KD Millipore (10 000r, 10 min). In parallel, 12 μL of thiolated oligonucleotide (100 μM DNA1 or DNA2) was reduced with 16 μL of 100 mM DTT in PBS for 1 h at 37 °C. Both the products were purified with a

100 KD Millipore at 10 000 r for 10 min. Then, the obtained anti-insulin-SMCC and reduced oligonucleotide were mixed in PBE (pH 7.4) containing 55 mM phosphate, 150 mM NaCl, and 5 mM EDTA to incubate overnight at 4 °C, the unreacted antibody and DNA were removed with the same ultrafiltration process, and the obtained DNA-Ab1 and DNA-Ab2 were collected in 50  $\mu$ L of PBE.

**Preparation of Signal DNA-CdTe QDs.** The synthesis of water-soluble MPA-modified CdTe QDs referred to the method reported previously (Supporting Information).<sup>44,45</sup> A volume of 100  $\mu$ L of 2  $\mu$ M CdTe QDs and 100  $\mu$ L of 20  $\mu$ M signal DNA containing 20 mM EDC and 10 mM NHS were mixed in PBS (pH 7.4) containing 55 mM phosphate, 150 mM NaCl, and 20 mM EDTA and left overnight in the dark under shaking, and the nonconjugated DNA was removed by ultrafiltration using a 100 KD Millipore (10 000 r, 10 min) to obtain the signal DNA-CdTe QDs probe,<sup>43,46</sup> which was kept at 4 °C prior to use.

**PAGE Analysis.** The 10% native PAGE was prepared in 1 $\times$  Tris-Borate-EDTA (TBE) buffer. The loading sample was subsequently mixed with 7  $\mu$ L of DNA sample, 1.5  $\mu$ L of 6 $\times$  loading buffer, and 1.5  $\mu$ L of UltraPower dye. The mixture was kept for 3 min and then applied onto the lane. The gel was run at 90 V for 90 min in 1 $\times$  TBE buffer and scanned with a Molecular Imager Gel Doc XR (Bio-Rad).

**Preparation of PEC Biosensor.** The ITO/TiO<sub>2</sub>/CdS electrode was first prepared (Supporting Information). A volume of 10  $\mu$ L of 1  $\mu$ M capture DNA was then mixed with 1  $\mu$ L of 1 mM TCEP in a 200  $\mu$ L PCR tube to incubate for 90 min at room temperature for reduction of disulfide bonds, and 10  $\mu$ L of 0.5  $\mu$ M reduced capture DNA solution was dropped directly onto the ITO/TiO<sub>2</sub>/CdS electrode and incubated for 2 h in the dark to form a self-assembled monolayer (SAM). The excess capture-DNA was removed via a room temperature-deionized water rinse ( $\sim$ 20 s). For avoiding the nonspecific adsorption, 10  $\mu$ L of 1 mM MCH solution was dropped on the electrode for 1 h to block the unmodified sites. After washing with Tris-HCl buffer and drying with the help of nitrogen, 10  $\mu$ L of 1  $\mu$ M DNA-Ab1 containing 0.5% BSA (w/v) was coated on the electrode overnight. After another washing step, the PEC biosensor was obtained and stored at 4 °C before use.

**Measurement Procedure.** Tris-HCl buffer (pH 7.4, 0.5 M NaCl) was supplemented with 0.5% BSA (w/v), 50 nM DNA-Ab2, 50 nM signal DNA-CdTe QDs, and serum samples. A volume of 10  $\mu$ L of the mixture was dropped on the PEC biosensor surface for 40 min incubation, followed by washing with Tris-HCl buffer (pH 7.4).<sup>47</sup> Afterward, the photoelectrochemical detection was performed at room temperature in 10 mL of PBS buffer (10 mM, pH 7.4) containing 0.1 M AA as a sacrificial electron donor. White light, with a spectral range of 200–2500 nm, was utilized as excitation light and was switched on and off at the interval of 10 s. The applied potential was selected as 0.0 V. The AA electrolyte was deaerated by pure nitrogen for 10 min before measurement.

## RESULTS AND DISCUSSION

**Characterization of DNA-QDs and PEC Biosensor.** The sensitized PEC signal resulted from the approach of signal DNA-CdTe QDs to the ITO/TiO<sub>2</sub>/CdS electrode. Thus, the preparation of signal DNA-CdTe QDs was first characterized with absorption and emission spectra (Figure 1). The appearance of the extra absorption peak at 260 nm indicated the successful biofunctionalization of QDs with the oligonu-

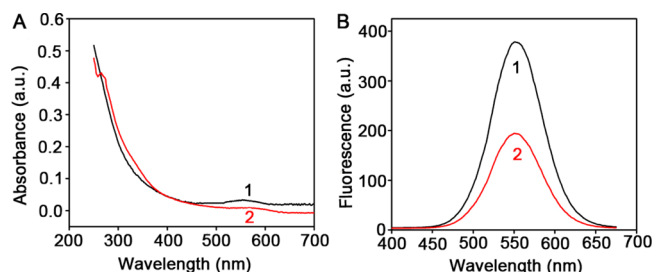


**Figure 1.** (A) Absorption and (B) emission spectra of (1) water-soluble MPA-capped CdTe QDs and (2) DNA-functionalized CdTe QDs.

cleotide, which led to lower quantum yield for the fluorescence emission due to the additional surface defects upon the association of the oligonucleotides,<sup>48</sup> thus the emission spectrum showed lower fluorescence intensity. The TEM image of CdTe-COOH QD film exhibited a uniform layer with the aggregate size of 4–6 nm (Figure S1). The average surface coverage of the oligonucleotide probes was estimated to be  $\sim$ 3 per QDs, measured by determining the amount of nontagged oligonucleotide probe spectroscopically.<sup>43</sup>

TiO<sub>2</sub> is of a wide energy band gap ( $\sim$ 3.2 eV), which absorbs the ultraviolet light ( $<$ 387 nm), while CdS has a narrow energy band gap ( $\sim$ 2.4 eV), and its absorption range extends to the wavelength of 550 nm. Therefore, the coupling of CdS with TiO<sub>2</sub> to form a TiO<sub>2</sub>/CdS hybrid structure evidently extends the absorption range, improves the utilization of light energy, and increases the photocurrent intensity.<sup>26</sup> In order to improve electron–hole recombination and further enhance the photocurrent intensity, several experiment conditions such as the concentration of TiO<sub>2</sub> suspension and coating number of CdS for the preparation of ITO/TiO<sub>2</sub>/CdS electrode with a successive ionic layer adsorption and reaction (SILAR) method were optimized. With the increasing concentrations of TiO<sub>2</sub>, the photocurrent of the ITO/TiO<sub>2</sub>/CdS electrode prepared with four cycles of CdS deposition showed the maximum value at 1.0 mg/mL (Figure 2A). In the low concentration range, the

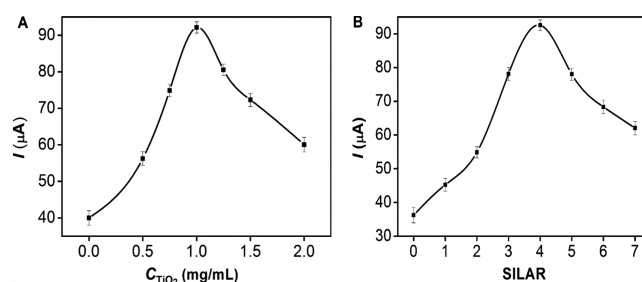


**Figure 2.** Effects of (A) concentration of TiO<sub>2</sub> suspension for preparation of ITO/TiO<sub>2</sub> electrode and (B) coating cycle number for CdS QD deposition on photocurrent of the ITO/TiO<sub>2</sub>/CdS electrode in 10 mL of PBS (10 mM, pH 7.4) containing 0.1 M AA at 0.0 V.

increase of TiO<sub>2</sub> concentration could offer a greater amount of TiO<sub>2</sub> on the electrode surface to absorb a greater amount of CdS. As a result, more light absorption occurred on the ITO/TiO<sub>2</sub>/CdS electrode and the photocurrent intensity increased. However, with the further increase of TiO<sub>2</sub> concentration, the diffusion resistance for electron motion in thicker TiO<sub>2</sub> film evidently increased due to more and more surface recombination centers on excessive TiO<sub>2</sub>,<sup>49</sup> leading to the gradually

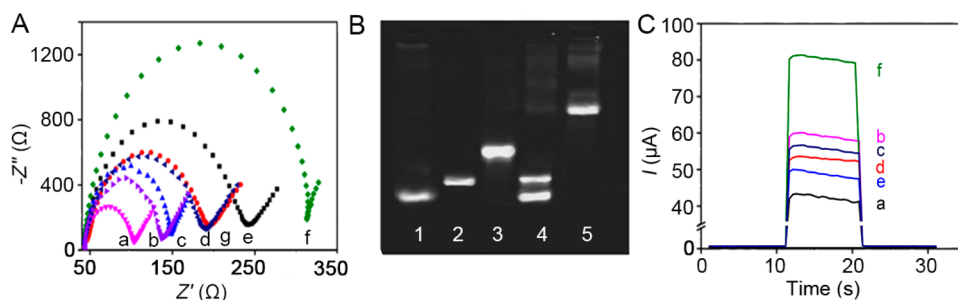


**Figure 3.** (A) EIS of (a) ITO/TiO<sub>2</sub>/CdS, (b) ITO/TiO<sub>2</sub>/CdS-capture DNA, (c) MCH-blocked ITO/TiO<sub>2</sub>/CdS-capture DNA, (d) electrode in spectrum reacted with 1 μM DNA-Ab1, (e) electrode in spectrum reacted with 0.4 nM insulin, (f) electrode in spectrum reacted with the mixture of 0.4 nM insulin, 50 nM DNA-Ab2, and 50 nM signal DNA-CdTe QDs, and (g) electrode in spectrum reacted with the mixture of 50 nM DNA-Ab2 and 50 nM signal DNA-CdTe QDs. (B) PAGE analysis. Lanes 1–5 represent DNA ladder marker, capture DNA, signal DNA, ref DNA, the mixture of capture DNA and signal DNA, and the mixture of capture DNA, signal DNA, and ref DNA at 10 nM, respectively. (C) Photocurrent responses of (a) ITO/TiO<sub>2</sub>, (b) ITO/TiO<sub>2</sub>/CdS, (c) ITO/TiO<sub>2</sub>/CdS-capture DNA, (d) MCH-blocked ITO/TiO<sub>2</sub>/CdS-capture DNA, (e) electrode in spectrum d incubated with the mixture of 50 nM DNA-Ab1 and 0.4 nM insulin, and (f) electrode in spectrum d incubated with 50 nM DNA-Ab1 and then the mixture of 0.4 nM insulin, 50 nM DNA-Ab2, and 50 nM signal DNA-CdTe QDs in 10 mL of PBS (10 mM, pH 7.4) containing 0.1 M AA at 0.0 V.

decreased photocurrent intensity. Thus, 1.0 mg/mL TiO<sub>2</sub> suspension was adopted for fabricating the electrode.

The deposition of CdS could be adjusted by the cycle number of SILAR. Similarly, at the TiO<sub>2</sub> concentration of 1.0 mg/mL, the photocurrent of ITO/TiO<sub>2</sub>/CdS electrode increased with the increase of deposition cycle number and reached the maximum at 4 cycles (Figure 2B). Afterward, the photocurrent decreased due to the increasing diffusion resistance for electron motion, which resulted from the excessive amount of CdS.<sup>50</sup> In order to achieve optimal signal amplification, four SILAR cycles for CdS deposition were chosen to fabricate the electrode.

The preparation of PEC biosensor and PECPA process were characterized with electrochemical impedance spectroscopy (EIS) (Figure 3A) in 0.1 M KCl containing 5 mM K<sub>3</sub>Fe(CN)<sub>6</sub> and K<sub>4</sub>Fe(CN)<sub>6</sub>.<sup>51</sup> Compared with the ITO/TiO<sub>2</sub>/CdS electrode (curve a), the capture DNA modified ITO/TiO<sub>2</sub>/CdS electrode showed a much larger electron transfer impedance  $R_{et}$  (curve b) due to the repel of negatively charged DNA to the [Fe(CN)<sub>6</sub>]<sup>3-/4-</sup>. After the surface was blocked with MCH,  $R_{et}$  increased (curve c). The capture of DNA-Ab1 on the electrode further increased the  $R_{et}$  due to the insulativity of protein (curve d). Similarly, the recognition of target protein to DNA-Ab1 resulted in the increasing impedance (curve e). In the presence of target protein, DNA-Ab2, and signal DNA-CdTe QDs, the formation of a cooperative complex among capture DNA, DNA-Ab1, target, DNA-Ab2, and signal DNA-CdTe QDs led to a larger increase of  $R_{et}$  (curve f). In contrast, no change of  $R_{et}$  was observed in the absence of target protein (curve g), which showed similar  $R_{et}$  to the PEC biosensor, the DNA-Ab1/capture DNA modified ITO/TiO<sub>2</sub>/CdS electrode. Overall, the successful fabrication of the biosensor and the proximity hybridization for PECPA of target protein according to Scheme 1 were demonstrated.

The proximity hybridization was further confirmed with a ref DNA to mimic the DNA-Ab1-target-DNA-Ab2 complex via PAGE analysis (Figure 3B). The ref DNA was designed to bring the signal and capture DNA in proximity for forming a cooperative complex. Capture DNA, signal DNA, and ref DNA exhibited individual clear band, respectively (lanes 1–3). In the absence of ref DNA, the mixture of capture DNA, and signal DNA displayed two bands at the same position as the capture DNA and signal DNA (lane 4), indicating no hybridization

occurred between capture DNA and signal DNA. Upon the addition of ref DNA to the mixture, a new band with a slow migration appeared (lane 5). This result should be contributed to the formation of proximate complex product of capture DNA-ref DNA-signal DNA.

**Feasibility of PECPA.** To acquire a cascade cosensitized structure, traditionally, different semiconductor materials need to be meticulously selected. As the photosensitizers, semiconductor quantum dots not only exhibit the merits of high absorption coefficient, delivery of hot electrons, and generation of multiple electron carriers but also possess the unique property of tunability of the band gap via varying particle size.<sup>52–54</sup> We hereby used a cosensitized structure for designing an ultrasensitive PECPA. The electron-transfer mechanism is shown in Figure S2.

In order to verify the feasibility of the designed sensitization strategy for signal amplification, photocurrent characterization of the PEC biosensing process was performed, as shown in Figure 3C. The ITO/TiO<sub>2</sub> electrode exhibited an evident photocurrent response (curve a). After the ITO/TiO<sub>2</sub> electrode was modified with CdS, the photocurrent increased obviously (curve b), which could be attributed to the photoelectrochemical properties of the semiconductor quantum dots. After capture DNA was assembled on the ITO/TiO<sub>2</sub>/CdS electrode, the photocurrent decreased moderately due to the relatively weak charge transfer of the DNA sequence (curve c). After MCH blocking, the photocurrent intensity decreased slightly (curve d), because the small organic molecule MCH partly obstructed AA to the electrode surface for reaction with the photogenerated holes. After the electrode was further incubated with DNA-Ab1 and insulin, both DNA-Ab1 and insulin were assembled on the capture DNA modified ITO/TiO<sub>2</sub>/CdS electrode, thus the photocurrent intensity decreased significantly due to their hindering effect on the access of AA and the charge transfer (curve e). However, the incubation of the capture DNA modified ITO/TiO<sub>2</sub>/CdS electrode with DNA-Ab1 and then the mixture of insulin, DNA-Ab2 and signal DNA-CdTe QDs led to the formation of a five-part complex at the electrode surface via proximity-dependent hybridization of the capture DNA and signal DNA-CdTe QDs, which brought CdTe QDs close to the ITO/TiO<sub>2</sub>/CdS surface and thus producing a significant enhancement of photocurrent (curve f). This process produced a quantity of electrons transferred from

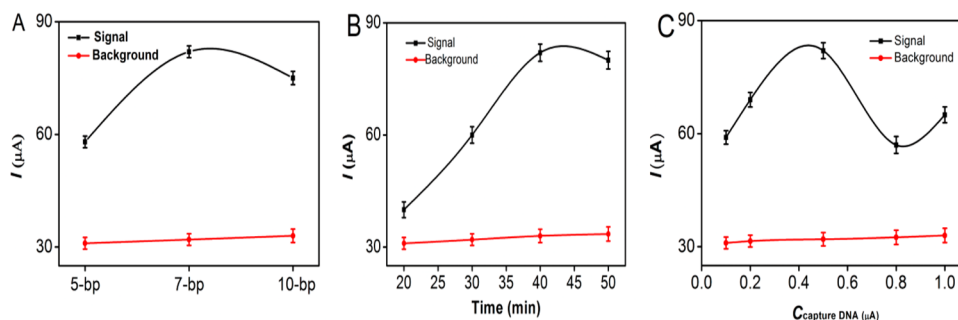


**Figure 4.** Effects of (A) complementary base number between capture DNA and signal DNA, (B) incubation time and (C) capture DNA concentration on photocurrent of photoelectrochemical sensor incubated with 0.4 nM insulin, 50 nM DNA-Ab2, and 50 nM signal DNA-CdTe QDs in 10 mL of PBS (10 mM, pH 7.4) containing 0.1 M AA at 0.0 V. Error bars represent standard deviations of three parallel experiments.

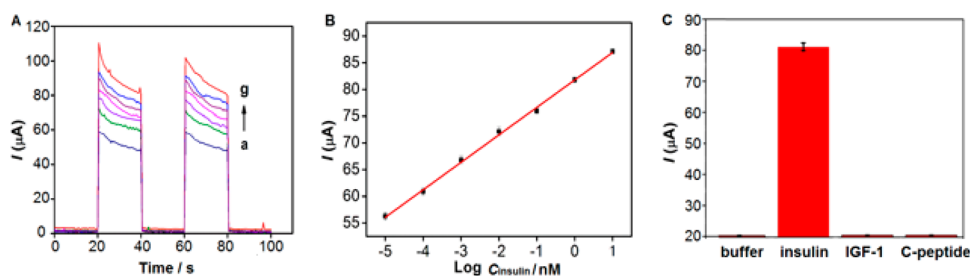


**Figure 5.** (A) Photocurrent responses of insulin at  $10^{-5}$  (a),  $10^{-4}$  (b),  $10^{-3}$  (c),  $10^{-2}$  (d),  $10^{-1}$  (e), 1 (f), and 10 nM (g). (B) Calibration curve for target insulin detection. (C) Selectivity of PECPA sensor incubated with buffer, 0.4 nM insulin, 4 nM IGF-1, and C-peptide. The error bars represent standard deviations of three parallel experiments.

CdTe QD to the ITO/TiO<sub>2</sub>/CdS electrode as shown in Scheme 1. Interestingly, the enhanced photocurrent depended on the amount of target protein insulin and thus providing a sensitive method for PECPA of insulin.

**Optimization of PECPA Conditions.** The photocurrent response of PECPA relies on simultaneous recognition of target protein by two DNA-antibodies to bring capture DNA and signal DNA-CdTe QDs in proximity hybridization. Hence the number of complementary bases between capture DNA and signal DNA-CdTe QDs and the incubation time were first optimized. Figure 4A illustrates the signals of the PECPA when using ref DNA to mimic the DNA-Ab1-target-DNA-Ab2 complex and bring signal DNA-CdTe QDs close to capture DNA with different numbers of complementary bases (G5, G7, and G10) for proximity hybridization. In the presence of 10 nM ref DNA, the photocurrent density increased with the increasing number of complementary bases and the maximum photocurrent occurred at 7 complementary bases. A longer sequence led to lower proximity ligation efficiency, which decreased the loading of CdTe quantum dots and the photocurrent. Thus, the capture DNA (G7) was selected for the subsequent experiments. The optimum incubation time was chosen as 40 min (Figure 4B).

The density of the immobilized capture DNA on biosensor surface affected its analytical performance. At an assembly time of 2 h for biosensor preparation, the maximum photocurrent occurred at the capture DNA concentration of 0.5  $\mu\text{M}$  (Figure 4C). Higher density of capture DNA would produce steric hindrance, which decreased the hybridization ability of the capture DNA with both DNA-Ab1 and signal DNA on biosensor surface. Hence, the biosensor was prepared with 10  $\mu\text{L}$  of 0.5  $\mu\text{M}$  capture DNA.

**Analytical Performance of PECPA.** The analytical performance of PECPA was characterized under the optimal

experimental conditions. With the increasing insulin concentration, the photocurrent increased correspondingly (Figure 5A). The plot of photocurrent vs the logarithm of insulin concentration showed a linearity in the range of 10 fM to 10 nM with a correlation coefficient of 0.9913 and a linear regression equation of  $I = 5.140 \log[C] + 81.784$  (Figure 5B). The limit of detection corresponding to a signal-to-noise ratio of 3 was 3.0 fM, which was lower than those of reported proximity immunoassays using complex amplification strategies.<sup>24,55</sup>

The selectivity of the PECPA method was tested against insulin-like growth factor 1 (IGF-1) and C-peptide, which is cosecreted with insulin into the bloodstream. As expected, the biosensor did not respond to both IGF-1 and C-peptide at higher concentrations (Figure 5C), and negligible response was observed in the interference solution, indicating few nonspecific binding. Furthermore, the photocurrent intensity of prepared biosensor did not show an obvious change after storage for 10 days at 4 °C. Thus, this biosensor had desirable longtime stability. The high sensitivity, wide linear range, easy operation, and good selectivity of the PECPA exhibited its great potential in point-of-care testing.

**Real Sample Analysis.** To evaluate the application potential and the analytical reliability of the proposed method, PECPA was applied to detect insulin in clinical serum samples. The assay results were compared with the reference values from the commercial electrochemiluminescent testing. The results showed acceptable agreement with relative errors less than 7.85% (Table S1), indicating good accuracy of the proposed method for the detection of clinical samples.

## CONCLUSION

This work develops a novel immunoassay strategy for photoelectrochemical proximity assay (PECPA) of target

protein. The simultaneous recognition of target protein by two DNA-antibodies can induce the proximity-dependent DNA hybridization of capture and signal DNA, which brings CdTe QDs near the ITO/TiO<sub>2</sub>/CdS electrode and thus produces a very strong photocurrent through the sensitization of CdTe QDs on the photoelectrochemical response of ITO/TiO<sub>2</sub>/CdS electrode. Using insulin as a target protein, the direct photoelectrochemical readout shows wide detectable range, high sensitivity, low detection limit, good selectivity, and acceptable accuracy. The PECPA possesses favorable expansibility for detection of other proteins with available antibody pairs, showing great potential in various settings, including medical diagnostics, biological research, and point-of-care testing.

## ■ ASSOCIATED CONTENT

### Supporting Information

The Supporting Information is available free of charge on the ACS Publications website at DOI: 10.1021/acs.analchem.6b02740.

Synthesis of CdTe-COOH QDs, preparation of ITO/TiO<sub>2</sub>/CdS electrode, electron-transfer mechanism, and assay results of clinical serum samples (PDF)

## ■ AUTHOR INFORMATION

### Corresponding Author

\*Phone/fax: +86-25-89683593. E-mail: hxju@nju.edu.cn.

### Notes

The authors declare no competing financial interest.

## ■ ACKNOWLEDGMENTS

We gratefully acknowledge the National Natural Science Foundation of China (Grants 21135002, 21361162002, and 21575083) and Priority Development Areas of The National Research Foundation for the Doctoral Program of Higher Education of China (Grant 20130091130005).

## ■ REFERENCES

- (1) Burtis, C. A.; Ashwood, E. R. *Tietz Textbook of Clinical Chemistry*; Saunders: Philadelphia, PA, 1999.
- (2) Rusling, J. F.; Kumar, C. V.; Gutkind, J. S.; Patel, V. *Analyst* **2010**, *135*, 2496–2511.
- (3) Akter, R.; Rahman, M. A.; Rhee, C. K. *Anal. Chem.* **2012**, *84*, 6407–6415.
- (4) Kattah, M. G.; Coller, J.; Cheung, R. K.; Oshidary, N.; Utz, P. J. *Nat. Med.* **2008**, *14*, 1284–1289.
- (5) Tavoosidana, G.; Ronquist, G.; Darmanis, S.; Yan, J.; Carlsson, L.; Wu, D.; Conze, T.; Ek, P.; Semjonow, A.; Eltze, E.; Larsson, A.; Landegren, U.; Kamali-Moghaddam, M. *Proc. Natl. Acad. Sci. U. S. A.* **2011**, *108*, 8809–8814.
- (6) Cheng, S. Y.; Shi, F.; Jiang, X. C.; Wang, L. M.; Chen, W. Q.; Zhu, C. G. *Anal. Chem.* **2012**, *84*, 2129–2132.
- (7) Weibrecht, I.; Lundin, E.; Kiflemariam, S.; Mignardi, M.; Grundberg, I.; Larsson, C.; Koos, B.; Nilsson, M.; Söderberg, O. *Nat. Protoc.* **2013**, *8*, 355–372.
- (8) Jung, J.; Lifland, A. W.; Zurla, C.; Alonas, E. J.; Santangelo, P. J. *Nucleic Acids Res.* **2013**, *41*, e12.
- (9) Nong, R. Y.; Gu, J. J.; Darmanis, S.; Kamali-Moghaddam, M.; Landegren, U. *Expert Rev. Proteomics* **2012**, *9*, 21–32.
- (10) Sano, T.; Smith, C. L.; Cantor, C. R. *Science* **1992**, *258*, 120–122.
- (11) Burbulis, I.; Yamaguchi, K.; Gordon, A.; Carlson, R.; Brent, R. *Nat. Methods* **2005**, *2*, 31–37.
- (12) Guo, Y. C.; Zhou, Y. F.; Zhang, X. E.; Zhang, Z. P.; Qiao, Y. M.; Bi, L. J.; Wen, J. K.; Liang, M. F.; Zha, J. B. *Nucleic Acids Res.* **2006**, *34*, e62.
- (13) Wang, T. W.; Lu, H. Y.; Lou, P. J.; Lin, F. H. *Biomaterials* **2008**, *29*, 4447–4454.
- (14) Yu, X.; Burgoon, M. P.; Shearer, A. J.; Gilden, D. H. *J. Immunol. Methods* **2007**, *326*, 33–40.
- (15) Barletta, J.; Bartolome, A.; Constantine, N. T. *J. Virol. Methods* **2009**, *157*, 122–132.
- (16) Nam, J. M.; Thaxton, C. S.; Mirkin, C. A. *Science* **2003**, *301*, 1884–1886.
- (17) Schweitzer, B.; Wiltshire, S.; Lambert, J.; O'Malley, S.; Kukanskis, K.; Zhu, Z.; Kingsmore, S. F.; Lizardi, P. M.; Ward, D. C. *Proc. Natl. Acad. Sci. U. S. A.* **2000**, *97*, 10113–10119.
- (18) Schweitzer, B.; Roberts, S.; Grimwad, B.; Shao, W. P.; Wang, M. J.; Fu, Q.; Shu, Q. P.; Laroche, I.; Zhou, Z.; Tchernev, V. T.; Christiansen, J.; Velleca, M.; Kingsmore, S. F. *Nat. Biotechnol.* **2002**, *20*, 359–365.
- (19) Ericsson, O.; Jarvius, J.; Schallmeiner, E.; Howell, M.; Nong, R. Y.; Reuter, H.; Hahn, M.; Stenberg, J.; Nilsson, M.; Landegren, U. *Nucleic Acids Res.* **2008**, *36*, e45.
- (20) Yan, J.; Song, S. P.; Li, B.; Zhang, Q. Z.; Huang, Q.; Zhang, H.; Fan, C. H. *Small* **2010**, *6*, 2520–2525.
- (21) Zhang, B.; Liu, B. Q.; Tang, D. P.; Niessner, R.; Chen, G. N.; Knopp, D. *Anal. Chem.* **2012**, *84*, 5392–5399.
- (22) Tong, L.; Wu, J.; Li, J.; Ju, H. X.; Yan, F. *Analyst* **2013**, *138*, 4870–4876.
- (23) Fredriksson, S.; Gullberg, M.; Jarvius, J.; Olsson, C.; Pietras, K.; Gustafsdottir, S. M.; Ostman, A.; Landegren, U. *Nat. Biotechnol.* **2002**, *20*, 473–477.
- (24) Gullberg, M.; Gustafsdottir, S. M.; Schallmeiner, E.; Jarvius, J.; Bjarnegård, M.; Betsholtz, C.; Landegren, U.; Fredriksson, S. *Proc. Natl. Acad. Sci. U. S. A.* **2004**, *101*, 8420–8424.
- (25) Kim, J.; Hu, J.; Sollie, R. S.; Easley, C. J. *Anal. Chem.* **2010**, *82*, 6976–6982.
- (26) Wang, G. L.; Xu, J. J.; Chen, H. Y.; Fu, S. Z. *Biosens. Bioelectron.* **2009**, *25*, 791–796.
- (27) Wang, G. L.; Yu, P. P.; Xu, J. J.; Chen, H. Y. *J. Phys. Chem. C* **2009**, *113*, 11142–11148.
- (28) Liang, M. M.; Liu, S. L.; Wei, M. Y.; Guo, L. H. *Anal. Chem.* **2006**, *78*, 621–623.
- (29) Haddour, N.; Chauvin, J.; Gondran, C.; Cosnier, S. *J. Am. Chem. Soc.* **2006**, *128*, 9693–9698.
- (30) Lee, Y. L.; Chi, C. F.; Liau, S. Y. *Chem. Mater.* **2010**, *22*, 922–927.
- (31) Li, S.; Wang, Y. H.; Gao, C. M.; Ge, S. G.; Yu, J. H.; Yan, M. J. *Electroanal. Chem.* **2015**, *759*, 38–45.
- (32) Fan, G. C.; Ren, X. L.; Zhu, C.; Zhang, J. R.; Zhu, J. J. *Biosens. Bioelectron.* **2014**, *59*, 45–53.
- (33) Ren, K. W.; Wu, J.; Yan, F.; Ju, H. X. *Sci. Rep.* **2014**, *4*, 4360.
- (34) Hu, J. M.; Wang, T. Y.; Kim, J. Y.; Shannon, C.; Easley, C. J. *J. Am. Chem. Soc.* **2012**, *134*, 7066–7072.
- (35) Bonham, A. J.; Hsieh, K.; Ferguson, B. S.; Vallée-Bélisle, A.; Ricci, F.; Soh, H. T.; Plaxco, K. W. *J. Am. Chem. Soc.* **2012**, *134*, 3346–3348.
- (36) Vallée-Bélisle, A.; Ricci, F.; Plaxco, K. W. *J. Am. Chem. Soc.* **2012**, *134*, 2876–2879.
- (37) Xia, F.; Zuo, X.; Yang, R.; White, R. J.; Xiao, Y.; Kang, D.; Gong, X.; Lubin, A. A.; Hsu, B. Y.; Plaxco, K. W. *J. Am. Chem. Soc.* **2010**, *132*, 8557–8559.
- (38) Rowe, A. A.; Chuh, K. N.; Lubin, A. A.; Miller, E. A.; Cook, B.; Hollis, D.; Plaxco, K. W. *Anal. Chem.* **2011**, *83*, 9462–9466.
- (39) Lubin, A. A.; Plaxco, K. W. *Acc. Chem. Res.* **2010**, *43*, 496–505.
- (40) Ren, K. W.; Wu, J.; Zhang, Y.; Yan, F.; Ju, H. X. *Anal. Chem.* **2014**, *86*, 7494–7499.
- (41) Liu, Y.; Tuleouva, N.; Ramanculov, E.; Revzin, A. *Anal. Chem.* **2010**, *82*, 8131–8136.
- (42) Zhang, Y. L.; Huang, Y.; Jiang, J. H.; Shen, G. L.; Yu, R. Q. *J. Am. Chem. Soc.* **2007**, *129*, 15448–15449.

- (43) Söderberg, O.; Gullberg, M.; Jarvius, M.; Ridderstråle, K.; Leuchowius, K.; Jarvius, J.; Wester, K.; Hydbring, P.; Bahram, F.; Larsson, L. G.; Landegren, U. *Nat. Methods* **2006**, *3*, 995–1000.
- (44) Zou, L.; Gu, Z. Y.; Zhang, N.; Zhang, Y. L.; Fang, Z.; Zhu, W. H.; Zhong, X. H. *J. Mater. Chem.* **2008**, *18*, 2807–2815.
- (45) Wang, R. F.; Wang, Y. L.; Feng, Q. L.; Zhou, L. Y.; Gong, F. Z.; Lan, Y. W. *Mater. Lett.* **2012**, *66*, 261–263.
- (46) Cheng, W.; Yan, F.; Ding, L.; Ju, H. X.; Yin, Y. B. *Anal. Chem.* **2010**, *82*, 3337–3342.
- (47) Ferapontova, E. E.; Olsen, E. M.; Gothelf, K. V. *J. Am. Chem. Soc.* **2008**, *130*, 4256–4258.
- (48) Gill, R.; Willner, I.; Shweky, I.; Banin, U. *J. Phys. Chem. B* **2005**, *109*, 23715–23719.
- (49) Kuang, D. B.; Ito, S.; Wenger, B.; Klein, C.; Moser, J. E.; Humphry-Baker, R.; Zakeeruddin, S. M.; Gratzel, M. *J. Am. Chem. Soc.* **2006**, *128*, 4146–4154.
- (50) Vogel, R.; Hoyer, P.; Weller, H. *J. Phys. Chem.* **1994**, *98*, 3183–3188.
- (51) Cao, Y.; Zhu, S.; Yu, J. C.; Zhu, X. J.; Yin, Y. M.; Li, G. X. *Anal. Chem.* **2012**, *84*, 4314–4320.
- (52) Kongkanand, A.; Tvrđy, K.; Takechi, K.; Kuno, M.; Kamat, P. V. *J. Am. Chem. Soc.* **2008**, *130*, 4007–4015.
- (53) Pandey, A.; Guyot-Sionnest, P. J. *J. Phys. Chem. Lett.* **2010**, *1*, 45–47.
- (54) Beard, M. C. *J. Phys. Chem. Lett.* **2011**, *2*, 1282–1288.
- (55) Heyduk, E.; Dummit, B.; Chang, Y. H.; Heyduk, T. *Anal. Chem.* **2008**, *80*, 5152–5159.